

Kinetic lattice gas model of collective diffusion in a one-dimensional system with long-range repulsive interactions

Magdalena A. Załuska-Kotur*

Institute of Physics, Polish Academy of Sciences, Aleja Lotników 32/46, 02-668 Warsaw, Poland

Zbigniew W. Gortel†

Department of Physics, University of Alberta, Edmonton, Alberta, Canada T6G 2J1

(Received 5 April 2006; published 6 July 2006)

Collective diffusion is investigated within the kinetic lattice gas model for systems of particles in one dimension with repulsive long-range interactions which are known to result in a staircaselike phase diagram with an infinite sequence of incompressible crystalline phases separated one from another by unstable compressible liquidlike phases. Using a recently proposed [Gortel and Załuska-Kotur, *Phys. Rev. B* **70**, 125431 (2004)] variational method, an analytic expression for the particle density dependence of the diffusion coefficient is derived in which commonly postulated static and kinetic factors are unambiguously identified. It is shown that while the static factor exhibits singular coverage dependence due to a sharp drop of compressibility when the system enters a crystalline phase, the kinetic factor may substantially modify this behavior. Depending on details of the activated state interactions controlling the migration kinetics the diffusion coefficient may also be singular or, at another extreme, it may be a continuously smooth function of density. In view of these observations recent results on efficient low temperature self-reorganization through devil's staircase phases in the dense Pb/Si(111)- $\sqrt{3} \times \sqrt{3}$ are discussed.

DOI: 10.1103/PhysRevB.74.045405

PACS number(s): 68.43.Jk, 66.30.Pa, 02.50.Ga, 66.10.Cb

I. INTRODUCTION

The collective or chemical diffusion of surface species involves jumps of adsorbed interacting particles from one binding site to another. The effectiveness of the surface diffusion in relation to that of other surface processes, like adsorption, desorption, chemical reactions, etc., determines the catalytic activity of the surface.^{1,2} Growth of nanostructures from beam deposited clusters is controlled by the cluster surface diffusion enabling them to grow into islands making surface diffusion a subject of interest in nanostructuring.³ The experimental progress in this field has been recently reviewed in Refs. 4–7. Collective diffusion is a complicated many-body problem which, with a few exceptions,^{8–11} is usually studied using a variety of Monte Carlo simulation methods. Early efforts were summarized in a classical review by Gomer¹² and, more recently, by Danani *et al.*¹³ and Alani-Nissila *et al.*¹⁴

Although diffusion within adsorbates is usually associated with diffusion in two dimensions, there exist experimentally studied and technologically important systems of this type which can adequately be modeled in one dimension. For example, static and dynamic properties of atoms confined in carbon nanotubes^{15–17} can be investigated using one-dimensional models; diffusion of Au or Si atoms on top of a Si(111)5×2-Au chain structure has one-dimensional character,^{18,19} etc. Recently, self-organization in truly two-dimensional systems,^{20,21} being the primary motivation of this work, has been shown to have essentially one-dimensional character.

Interactions between the neighboring atoms modify rates of atomic jumps leading to the coverage dependent diffusion coefficient (the coverage θ is defined as a ratio of the actual particle density to its maximum value reached when each

adsorption site is occupied). The interactions affect the coverage dependence of diffusion also through the structural transformations within the adsorbate layer which favor different geometrical configurations within the adsorbate at different coverages. It is usually understood that interparticle interactions influence diffusion in two ways:²² by affecting the thermodynamic (static) properties of the system and by modifying the kinetics of motion of particles. For example, in a case of an adsorbate, the thermodynamic properties are fully determined by “ground state interactions” between non-activated particles. These interactions affect also kinetics of diffusion but, in addition, also interactions between an activated particle and surrounding it nonactivated ones, i.e., the “activated state interactions” play an important role in kinetics. A distinct role played by kinetics and thermodynamics in diffusion is often emphasized by writing the collective diffusion coefficient as a product^{12,23}

$$D(\theta) = D_J(\theta) \left(\frac{\partial(\mu/k_B T)}{\partial \ln \theta} \right)_T \quad (1)$$

of the jump rate diffusion coefficient $D_J(\theta)$, accounting for the effective jump kinetics in an interacting system, and a “thermodynamic factor” directly related to the isothermal compressibility or, equivalently, to the equilibrium mean square particle number fluctuation. While the thermodynamic factor can be in principle modeled easily, modeling the jump rate diffusion coefficient is more difficult. In our past work^{24,25} we have avoided postulating the factorization of the diffusion coefficient choosing, instead, to evaluate the collective diffusion coefficient as a whole—in “one shot.” In this way, possibly inconsistent approximation schemes in evaluating each factor separately are avoided. We follow the same approach also in this work but, in addition, we explic-

itly identify in our expressions both the kinetic and the thermodynamic factors. This allows one to determine unambiguously which of the two factors is responsible for observed structures in the $D(\theta)$ dependence, e.g., due to the structural organization of the adsorbate. It is important in view of possible cancellations when both factors are multiplied by each other.

Diffusion on a lattice is particularly well-suited for a “one shot” approach. A clear separation of time scales between elementary transition processes (particle jumps between adsorption sites) and the time lapse between successive transitions (the sequence of which leads to the observed diffusion) allows one to treat one particle jump at a time, consider them to be statistically independent, and invoke the Markovian hypothesis that the present state of the system is fully determined by its state at one past time rather than by its entire past history. Consequently, the kinetics of the microscopic states of the system, labeled by $\{c\}$'s, is governed by a Markovian master equation for the probability $P(\{c\}, t)$ that a microstate $\{c\}$ of the system occurs at time t

$$\frac{d}{dt}P(\{c\}, t) = \sum_{\{c'\}} [W(\{c\}, \{c'\})P(\{c'\}, t) - W(\{c'\}, \{c\})P(\{c\}, t)], \quad (2)$$

from which the collective diffusion coefficient can be directly extracted as shown in Refs. 24 and 25. In Eq. (2), $W(\{c\}, \{c'\})$ denotes a transition probability per unit time that the microstate $\{c'\}$ changes into $\{c\}$ due to a particle jump of a particle from an occupied site to an unoccupied neighboring one. It must be emphasized that modeling kinetics of diffusion, here, proposing model expressions for the rates $W(\{c\}, \{c'\})$, requires going beyond modeling necessary to investigate the equilibrium properties for which only the ground state interactions are necessary. The rates must be compatible with these interactions (through, e.g., detailed balance conditions) but their specification requires modeling the activated state interactions. While such interactions were ignored in early numerical simulations of diffusion, their importance is strongly emphasized in recent simulations of diffusion on generic triangular^{26,27} and square lattices²⁸ and systems intended to account for diffusion in the O/W(110) system.^{29,30} More recently, these interactions have been found crucial in accounting for diffusion of H on Pt(111) surfaces.³¹

Recent experiments^{20,21} on adsorbate self-organization in Pb/Si(111) indicate that by varying adsorbate coverage by as little as $\Delta\theta \sim 0.006$ ML the adsorbate reorganizes, without the need of thermal annealing, from one structural phase to another one, distinctively different from the former and extending over macroscopic distances (~ 0.5 mm). A succession of several phases was observed within the interval from 1/5 to 1/3 above monolayer coverage. The interpretation provided in Refs. 20 and 21 is that this system is an example of the devil's staircase system showing a high degree of self-organization driven by long-range adatom-adatom interactions. Phase diagrams for best known devil's staircase systems in one dimension in which every atom interacts with

every other one via distance-dependent forces were theoretically and numerically investigated in Refs. 32 and 33 and reviewed in Ref. 34. $T=0$ plots of coverage θ vs chemical potential μ in such systems have a fractal structure and consist of horizontal plateaus at rational values of coverage, $\theta = m/n$, where $m \leq n$ are integers. At such a coverage the system is in a crystalline phase with the elementary cell consisting of n equidistant adsorption sites (with a being the distance between neighboring sites) occupied by m atoms with at most two, differing by a , possible values of a distance between nearest atoms. Width $\Delta\mu$ of each plateau determines stability of a particular phase—the most stable one, with the largest $\Delta\mu$, corresponds to $\theta=1/2$ for which every second adsorption site is occupied. The fact that upon infinitesimally small coverage change the reorganization of the system occurs without annealing faster than it could be observed may be interpreted as an indication that the collective diffusion coefficient, as a function of coverage, has sharp maxima at rational values of θ . The maximum values are larger for more stable phases.

Diffusion in a true devil's staircase system has not been theoretically investigated yet and it seems to be a formidable mathematical task. In this work we limit our attention to a simpler system in which each atom interacts only with its first neighbor to its left and right via a distance-dependent force (a procedure referred to in Ref. 35 as the NN-approximation). In particular, it was shown in Ref. 35 that for long-range repulsive interactions between the neighbors (satisfying certain conditions, cf. Sec. II B) the interparticle correlations are capable of producing with increasing pressure a continuous transition from a weakly nonideal gas to “crystalline” phases with coverages $\theta=1/\ell$, where ℓ is an integer (the actual particle density is θ/a where a is the lattice constant). Transitions through the crystalline states with different ℓ occur via narrow regions of a liquidlike state. Our goal is to investigate how the collective diffusion coefficient varies when such a system passes through its different crystalline phases. To differentiate from the true devil's staircase system and motivated by a shape of its isotherms (cf. Fig. 1) we refer to the system resulting from its NN-approximation as an (ordinary) staircase system. We will see that although the diffusion coefficient static factor exhibits singular coverage dependence due to a sharp drop of the static compressibility when the system enters a crystalline phase, the kinetic factor can substantially modify this behavior resulting in $D(\theta)$ being either a singular or continuously smooth function of θ depending on details of the activated state interactions controlling adatom migration kinetics.

In order to investigate diffusion in a staircase system the recently developed analytic approach^{24,25} to diffusion in a one-dimensional lattice gas system must be generalized. An extra perhaps minor benefit coming from this generalization is that all analytic results for all short-range interaction models considered in Refs. 24 and 25 are quickly recovered in a more transparent way than in the original papers.

The paper is organized as follows. Theoretical basis is provided in Sec. II in which we summarize first the theoretical method used (Sec. II A), summarize thermodynamic properties of the staircase system (Sec. II B), unambiguously identify and investigate the diffusion coefficient static factor

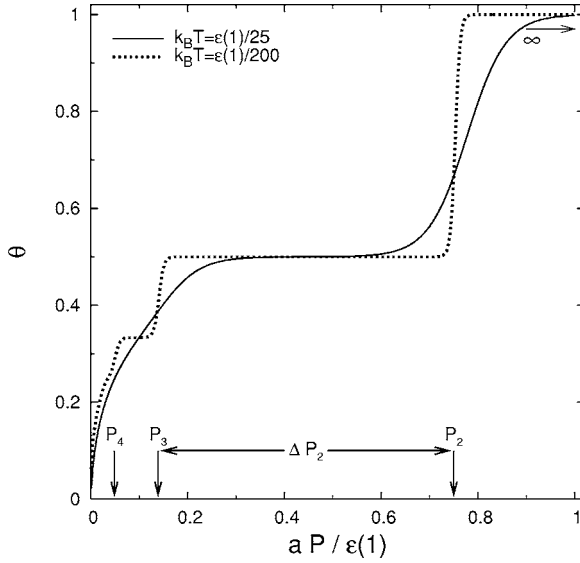


FIG. 1. Isotherms for the system with the NN-pair interaction given in Eq. (21) for “low” and “high” temperature. The characteristic pressure values P_2 , P_3 , and P_4 and the pressure interval ΔP_2 are defined in Eqs. (19) and (20), respectively. Pressures above roughly $P_2 + k_B T/a$ correspond to $\theta=1$ due to the impossibility of occupying an adsorption site by more than one particle.

(Sec. II C), and derive the expression for the kinetic factor (Sec. II D). After testing our approach by reproducing already known results^{24,25} (Secs. III A and III B) we concentrate in Sec. III C on the staircase system with long-range interactions for which the diffusion coefficient kinetic factor is obtained for several models of the migration kinetics corresponding to different activated state interactions (Secs. III C 1–III C 3). Numerical results are presented and discussed in Sec. IV and some comments on possible generalizations for the true devil’s staircase system are made in Sec. V. Section VI is devoted to final comments, conclusions, and summary.

II. THEORY

A. Theoretical method—summary

We summarize here the theoretical method used to extract the collective diffusion coefficient from the microscopic Master equation (2). We consider a one-dimensional lattice consisting of L adsorption sites which can be occupied by particles, N in total, with no more than one particle at a given adsorption site. The lattice constant is a . A microstate $\{c\}$ is identified by a set of N numbers

$$\{c\} = [X; m_1, m_2, \dots, m_{N-1}] \equiv [X; \{m\}], \quad (3)$$

where $X = na$ ($n = 0, \pm 1, \pm 2, \dots, \pm \infty$) is a position of one of the particles, referred to as the reference particle, and m_i is an integer indicating the distance, in units of the lattice constant a , of the i th particle away from the reference particle. The set $\{m\} = [m_1, m_2, \dots, m_{N-1}]$ —referred to as a configuration—accounts for the relative arrangement of particles in a given microstate. With periodic boundary conditions the lattice po-

sitions X and $X + La$ are equivalent: it is convenient to consider all L sites to be arranged along a circumference of a circle of length La . Two possible directions along the line will be referred to either as clockwise (from left to right) or counterclockwise (from right to left). Choosing the reference particle to be the leftmost one in the microstate and labeling the remaining particles with integers $i = 1, 2, \dots, N-1$ in the order in which they are encountered going from the reference particle in the clockwise (right) direction results in the set $\{m\}$ to be ordered as follows:

$$1 \leq m_1 < m_2 < \dots < m_i < \dots < m_{N-1} \leq L-1. \quad (4)$$

For example, if $N=3$ then the microstate $\circ\circ\bullet\bullet\circ\circ\bullet\circ\circ\dots$ is identified as $[X; m_1, m_2] = [2a; 1, 4]$ and the corresponding configuration is $\{m\} = [1, 4]$.

The transition rates do not depend on the positions of the reference particle in both configurations involved but only on the relative position of the hopping particle with respect to all other particles so $W(\{c\}, \{c'\}) = W_{\{m\}, \{m'\}}$. This allows one to take the lattice Fourier transform of the Master equations to convert them into the rate equations in k -space

$$\frac{d}{dt} P_{\{m\}}(k, t) = \sum_{\{m'\}} M_{\{m\}, \{m'\}}(k) P_{\{m'\}}(k, t), \quad (5)$$

where $P_{\{m\}}(k, t)$ is the lattice Fourier transform of $P([X; \{m\}], t)$ and

$$M_{\{m\}, \{m'\}}(k) = F_{\{m\}, \{m'\}}(k) W_{\{m\}, \{m'\}} - \delta_{\{m\}, \{m'\}} \sum_{\{m''\}} W_{\{m''\}, \{m'\}} \quad (6)$$

are matrix elements of the k -space rate matrix $\mathbb{M}(k)$. The factor $F_{\{m\}, \{m'\}}(k)$ is equal to 1 except when the configuration $\{m\}$ is obtained from $\{m'\}$ as a result of a jump of the reference particle. In such case it is equal to $\exp(ika)$ for the clockwise or $\exp(-ika)$ for the counterclockwise jump. The rate matrix is, in general, non-Hermitian because the hopping rates between a pair of sites in opposite directions are not necessarily the same. Consequently, a left eigenvector is not equal to the Hermitian conjugate of the corresponding right eigenvector. Instead, a simple relation exists between the $\{m\}$ th component of the left eigenvector, $\tilde{e}_{\{m\}}(k)$, and the component, $e_{\{m\}}(k)$, of the corresponding right eigenvector

$$e_{\{m\}}(k) = P_{\{m\}}^{\text{eq}} e_{\{m\}}^*(k), \quad (7)$$

as a consequence of the detailed balance condition satisfied by the rates $W_{\{m\}, \{m'\}}$. Here $P_{\{m\}}^{\text{eq}}$ is the probability of the configuration $\{m\}$ in equilibrium, i.e., it is the $\{m\}$ th component of the right eigenvector of $\mathbb{M}(k=0)$ corresponding to its vanishing eigenvalue, $\lambda_D(k=0) = 0$. The eigenvalue $-\lambda_D(k)$ of the rate matrix $\mathbb{M}(k)$ which vanishes in the limit $k \rightarrow 0$, referred to as the diffusive eigenvalue, is of particular interest because the collective diffusion coefficient can be evaluated directly from it as follows:

$$D(\theta) = \lim_{k \rightarrow 0} \frac{\lambda_D(k)}{k^2}. \quad (8)$$

For the lattice gas, the limit means $ka \ll 1$.

If all components $\tilde{e}_{\{m\}}^*(k)$ of the left diffusive eigenvector of $\mathbb{M}(k)$ and the equilibrium probabilities $P_{\{m\}}^{\text{eq}}$ are known then the diffusive eigenvalue can be evaluated as a ratio

$$-\lambda_D(k) = \mathcal{M}(k)/\mathcal{N}(k) \quad (9)$$

of the “expectation value numerator”

$$\begin{aligned} \mathcal{M}(k) &= \sum_{\{m\}, \{m'\}} \tilde{e}_{\{m\}}^*(k) M_{\{m\}, \{m'\}}(k) P_{\{m'\}}^{\text{eq}} \tilde{e}_{\{m'\}}^*(k) \\ &\quad \text{no rep} \\ &= \sum_{\{m\}, \{m'\}} P_{\{m'\}}^{\text{eq}} W_{\{m\}, \{m'\}} \\ &\quad \times |F_{\{m\}, \{m'\}}(k) \tilde{e}_{\{m'\}}^*(k) - \tilde{e}_{\{m\}}^*(k)|^2, \end{aligned} \quad (10)$$

to the “normalization denominator”

$$\mathcal{N}(k) = \sum_{\{m\}} P_{\{m\}}^{\text{eq}} |\tilde{e}_{\{m\}}^*(k)|^2. \quad (11)$$

The second result in Eq. (10) is obtained from the first one after Eq. (6) is used together with the detailed balance condition. The comment “no rep” above the sum means that each configuration pair $\{m\}, \{m'\}$ for which $W_{\{m\}, \{m'\}} \neq 0$ appears in the summation only once—such term accounts for both transitions, from $\{m'\}$ to $\{m\}$ and back. The equilibrium probabilities are normalized:

$$\sum_{\{m\}} P_{\{m\}}^{\text{eq}} = 1, \quad (12)$$

and summing over configurations in Eqs. (10)–(12) the ordering condition (4) must be obeyed.

Equations (8)–(11) are the theoretical starting point for all applications. We shall see later that $\mathcal{N}(k=0)$ is directly related to the thermodynamic factor in Eq. (1) while the $ka \ll 1$ limit of $\mathcal{M}(k)/k^2$ is a kinetic factor proportional to the jump rate diffusion coefficient $D_J(\theta)$ in Eq. (1). Its evaluation requires specifying a model for the particle jump rates—they must satisfy the detailed balance condition. In addition, $\tilde{e}_{\{m\}}^*(k)$ and $P_{\{m\}}^{\text{eq}}(k)$ are needed in both the numerator $\mathcal{M}(k)$ and the denominator $\mathcal{N}(k)$. Generally, they are not known and plausible “variational” candidates must be proposed. It is important to note that whatever approximate expressions are proposed, the choice is the same for both the static and the kinetic factor. This is not necessarily the case in approaches in which both factors are modeled independently. One of the requirements for the diffusive left eigenvector, due to the overall particle number conservation, is that all its components $\tilde{e}_{\{m\}}^*(k)$ tend to be the same limit for $ka \ll 1$ with linear ka corrections which may be different for different configurations $\{m\}$.

Similarly like in all our previous one-dimensional applications^{24,25} we propose the following approximation for $\tilde{e}_{\{m\}}^*(k)$:

$$\tilde{e}_{\{m\}}^*(k) \equiv \tilde{e}_{m_1, m_2, \dots, m_{N-1}}^*(k) \approx 1 + \sum_{j=1}^{N-1} e^{-ikam_j}. \quad (13)$$

Note that each of the $N-1$ terms in the sum corresponds to one of the $N-1$ particles. The initial “1” may be considered to be a contribution $\exp(-ikam_0)$ due to the reference particle with $m_{j=0}=0$. This is the simplest possible proposition motivated by the fact that the expression on the right-hand side of Eq. (13) is *exact* for the lattice gas in which all the particle jump rates are the same (and the only restriction is the site blocking preventing their double occupancy). The accuracy of the ansatz given in Eq. (13) was tested with good results in Ref. 25 against the results of Monte Carlo simulations for a one-dimensional model with short-range interactions. Sometimes, like in our recent application to a two-dimensional lattice gas,³⁶ it is necessary to propose more sophisticated candidates for $\tilde{e}_{\{m\}}^*(k)$.

B. Thermodynamics

For the interacting lattice gas, two particles at the lattice positions al_i and al_j contribute the potential energy $\varepsilon(l_i - l_j)$ to the total energy of the system. Following Ref. 35 we consider systems with the pair potential energy $\varepsilon(\ell)$ declining rapidly with ℓ . This implies that one can neglect the next-nearest-particle interactions but account for pair interactions between neighbors no matter how large the intrapair separation $a\ell$ is. The devil’s staircase system^{32,34} would result if interactions between any two particles were considered. Limiting the interactions to first neighbors only is referred to as the NN-approximation in Ref. 35. The total interaction energy in the resulting “staircase” system is $\sum_{\ell} n_{\ell} \varepsilon(\ell)$ where n_{ℓ} is the number of NN-pairs of length ℓ (in units of a) and only ℓ ’s satisfying the condition $\sum_{\ell} \ell n_{\ell} = L$ are admitted in the sum. Such restriction leads to impossibly complicated combinatorics which can be avoided by letting ℓ vary from 0 to ∞ and keeping, instead, the system under fixed external pressure P (in 1D it is just an external force) which is determined by the condition that the mean NN-pair length $\langle \ell \rangle$ is equal to the inverse of the actual coverage $\theta = N/L$. In such case a probability of a pair of length ℓ is³⁵

$$p_{\ell}(P, T) = Z_1^{-1}(P, T) e^{-\beta \tilde{\varepsilon}(\ell, P)}, \quad (14)$$

where

$$\tilde{\varepsilon}(\ell, P) = \varepsilon(\ell) + aP\ell \quad (15)$$

and

$$Z_1(P, T) = \sum_{\ell=1}^{\infty} e^{-\beta \tilde{\varepsilon}(\ell, P)} \quad (16)$$

is a single NN-pair isothermal-isobaric partition function.

Equations (14)–(16) allow one to determine the thermodynamic properties of the system. In particular, the equation of state, relation between coverage, pressure, and temperature are obtained by evaluating the mean NN-pair length

$$\langle \ell \rangle = Z_1^{-1}(P, T) \sum_{\ell=1}^{\infty} \ell e^{-\beta \bar{\varepsilon}(\ell, P)} = - \frac{1}{\beta a} \left(\frac{\partial \ln Z_1}{\partial P} \right)_T, \quad (17)$$

and identifying it with $1/\theta$. Another physical quantity of interest is the isothermal compressibility K_T . Using Eqs. (14)–(17) one gets

$$K_T \equiv - \frac{1}{N \langle \ell \rangle} \left(\frac{\partial N \langle \ell \rangle}{\partial P} \right)_{T, N} = \beta a \frac{\langle \ell^2 \rangle - \langle \ell \rangle^2}{\langle \ell \rangle}. \quad (18)$$

There are no formal restrictions on the pair interaction energy $\varepsilon(\ell)$. In particular, the standard Ising-like system corresponds to $\varepsilon(1)=J$ and $\varepsilon(\ell \geq 2)=0$ with repulsive ($J>0$) or attractive ($J<0$) interactions between particles at neighboring sites.

Particularly interesting is the case in which $\varepsilon(\ell)$ corresponds to repulsive interaction, is a convex function of ℓ , and declines faster than $1/\ell$. It is shown in Ref. 35 that in such case the effect of interparticle correlations is controlled by the product $\gamma = \beta a P$. Namely, for $\gamma \ll 1$ (low pressure and/or high temperature) the system is in the low coverage ideal gas limit with the standard equation of state $\theta = \beta a P$. In the opposite high pressure and/or low temperature limit, $\gamma \gg 1$, the thermodynamic limit depends on whether the function $\bar{\varepsilon}(\ell, P)$ has a minimum or not as a function of the discrete variable ℓ . In the former case, when the pressure is lower than $P_C \equiv P_2$, where

$$aP_{q+1} = \varepsilon(q) - \varepsilon(q+1), \quad q = 1, 2, \dots, \quad (19)$$

the plot of θ vs P dependence has a staircaselike shape. It is characterized by broad plateaus extending roughly over intervals (P_{q+1}, P_q) of width

$$a\Delta P_q \equiv a(P_q - P_{q+1}) = \varepsilon(q-1) - 2\varepsilon(q) + \varepsilon(q+1), \quad (20)$$

in which θ does not depend on P and has a value $1/q$: the lattice gas forms an incompressible crystal with a lattice constant aq . When the increasing pressure passes through P_q then the coverage increases rapidly from the plateau value $1/q$ to $1/(q-1)$ while the system passes through a liquidlike phase with a finite compressibility over a narrow pressure interval of width of the order of $k_B T/a$. This behavior can be easily understood: within the plateau region, for pressures P such that $P_{q+1} < P < P_q$, only one term with $\ell=q$, corresponding to the lowest value of $\bar{\varepsilon}(\ell, P)$ makes a major contribution to the sums in Eqs. (16) and (17). Within a narrow transition region for $P \approx P_{q+1}$ we have $\bar{\varepsilon}(q, P) \approx \bar{\varepsilon}(q+1, P)$ so two terms, with $\ell=q$ and $q+1$, contribute roughly equally. For pressures higher than $P_C = P_2$ the coverage reaches the maximum value of $\theta=1$.

These properties are illustrated in Fig. 1 for the long-range interaction

$$\varepsilon(\ell) = \frac{\varepsilon(1)}{\ell^2}. \quad (21)$$

C. The static factor

We are ready to evaluate, within the NN-approximation, the denominator $\mathcal{N}(k; L, N)$ given in Eq. (11). The calculation proceeds roughly along the lines of a similar calculation in Appendix F of Ref. 24 leading to Eq. (46) there. In short, substituting Eq. (13) for $\bar{\varepsilon}_{\{m\}}(k)$ and evaluating $|\dots|^2$ results in 1's added together N times [when $\exp(ikam_j)$ is multiplied by its complex conjugate] and $N(N-1)$ terms like $\exp[ika(m_s - m_j)]$ —with all possible distances between particles appearing in the exponents. Rearranging the summation indices and using the normalization condition (12) one arrives at the analog of Eq. (F2) in Ref. 24

$$\mathcal{N}(k; L, T, N) = N \left(1 + \sum_{\{m\}} P_{\{m\}}^{\text{eq}} \sum_{j=1}^{(N-1)/2} [e^{ikam_j} + e^{-ikam_j}] \right). \quad (22)$$

Note that in Eq. (22) the two exponents correspond, respectively, to the distances from the reference particle being counted for half of the particles in the clockwise direction and for the remaining half in the counterclockwise direction. The periodic boundary condition, $\exp(ikaL)=1$, is essential in rearranging the original sums into the above form.

The sum over $\{m\}$ is in Eq. (22) over all possible microscopic configurations so a particular distance am_j in one configuration is going to appear also in a different configuration, possibly corresponding to a different j . Consequently, the order of summations can be reversed and we get

$$\mathcal{N}(k; L, T, N) = N \left(1 + \sum_{j=1}^{(N-1)/2} [\langle e^{ikam_j} \rangle_{LTN} + \langle e^{-ikam_j} \rangle_{LTN}] \right). \quad (23)$$

Here,

$$\langle e^{ikam_j} \rangle_{LTN} = \sum_{\{m\}} P_{\{m\}}^{\text{eq}} e^{ikam_j} \quad (24)$$

is a mean value of $\exp(ikam_j)$ (for the j th particle counting clockwise from the reference particle) evaluated by averaging over all configurations of the lattice gas consisting of N particles distributed among L adsorption sites. Such average cannot be calculated analytically and is replaced here with $\langle e^{ikam_j} \rangle_{PT}$, the average over all possible configurations of the lattice gas of N particles distributed among an undetermined number of lattice sites subjected to the external pressure P (we omit N in the subscript anticipating that the mean is an intensive quantity). Consequently, we evaluate $\mathcal{N}(k; P, T, N)$ rather than $\mathcal{N}(k; L, T, N)$.

Consider $j=1$, i.e., we focus attention on the first particle in the clockwise direction away from the reference particle. It can either be at a distance a from it, i.e., $m_1=1$, or at a distance $2a$, corresponding to $m_1=2$, or, in general at a distance $a\ell$ and then $m_1=\ell$. In each case the reference particle forms a NN-pair with the $j=1$ particle, all remaining NN-pairs can have an arbitrary length so the situations listed above occur with probabilities $p_1(P, T)$, $p_2(P, T)$, or $p_\ell(P, T)$, respectively, defined in Eq. (14). Note that the probabilities do not depend on N so

$$\langle e^{ikam_1} \rangle_{PT} = \sum_{\ell=1}^{\infty} p_{\ell}(P, T) e^{ika\ell} \quad (25)$$

depends on P (and T) but not, as anticipated, on N .

For $j=2$ the simplest possible configuration is $\bullet\bullet\bullet\times\times\cdots$ (the leftmost \bullet denotes the reference particle, while \times denotes a site which can either be empty or occupied by any particle with $j>2$). This configuration corresponds to $m_2=2$ and contributes $\exp(2ika)p_1p_1$ to $\langle \exp(ikam_2) \rangle_{PT}$. Then, for $m_2=3$ we have $\bullet\bullet\bullet\circ\bullet\times\times\cdots$, or $\bullet\circ\bullet\bullet\times\times\cdots$ (with \circ denoting an empty site). The probabilities are p_1p_2 and p_2p_1 so the contribution is $\exp(3ika) \times (p_1p_2 + p_2p_1)$. For $m_2=4$ there are three possibilities: $\bullet\bullet\circ\circ\bullet\times\cdots$, $\bullet\circ\bullet\circ\bullet\times\cdots$, or $\bullet\circ\circ\bullet\bullet\times\cdots$ and the contribution is $\exp(4ika)(p_1p_3 + p_2p_2 + p_3p_1)$. The pattern continues and the result is

$$\begin{aligned} \langle e^{ikam_2} \rangle_{PT} &= \sum_{n=2}^{\infty} \sum_{\ell=1}^{n-1} e^{ikna} p_{\ell}(P, T) p_{n-\ell}(P, T) \\ &= \sum_{\ell=1}^{\infty} \sum_{\ell'=1}^{\infty} e^{ik(\ell+\ell')} p_{\ell}(P, T) p_{\ell'}(P, T) \\ &= (\langle e^{ikam_1} \rangle_{PT})^2. \end{aligned} \quad (26)$$

This result can be easily generalized for any j :

$$\langle e^{ikam_j} \rangle_{PT} = (\langle e^{ikam_1} \rangle_{PT})^j. \quad (27)$$

Using Eq. (26) in Eq. (23) [with $\langle \cdots \rangle_{LTN}$ replaced with $\langle \cdots \rangle_{PT}$] one ends up with a sum of a geometric progression summed up to $j=(N-1)/2$. Extending this to ∞ for $N \gg 1$ we get

$$\mathcal{N}(k; P, T, N) = N \left[1 + \frac{\langle e^{ikam_1} \rangle_{PT} (1 - \langle e^{ikam_1} \rangle_{PT}) + \text{c.c.}}{|1 - \langle e^{ikam_1} \rangle_{PT}|^2} \right], \quad (28)$$

which depends on N only through the multiplicative factor.

To get $\mathcal{N}(k=0; P, T, N)$ it is convenient to expand the exponential terms in Eq. (25) in a power series of ka . One gets

$$\langle e^{ikam_1} \rangle_{PT} = \sum_{s=0}^{\infty} \frac{(ka)^s}{s!} \langle \ell^s \rangle, \quad (29)$$

where $\langle \ell^s \rangle$ without subscripts denotes averaging with the NN-pair length probabilities, like in Eq. (17). Inserting this into Eq. (28) it is necessary to keep terms up to $s=2$. The result is

$$\begin{aligned} \mathcal{N}(k=0; P, T, N) &= N \frac{\langle \ell^2 \rangle - \langle \ell \rangle^2}{\langle \ell \rangle^2} = N \frac{K_T}{\beta a \langle \ell \rangle} \\ &= N \left[\left(\frac{\partial(\mu/k_B T)}{\partial \ln \theta} \right)_T \right]^{-1}, \end{aligned} \quad (30)$$

where K_T and μ are the isothermal compressibility and the chemical potential, respectively. To get the second result in Eq. (30), Eq. (18), relating the isothermal compressibility to the mean square NN-pair length fluctuation, was used. These relations demonstrate that the inverse of the collective diffu-

sion denominator $\mathcal{N}(k=0)$ is, up to a factor N , equal to the thermodynamic factor appearing in Eq. (1).

It was argued already³⁵ that for pressures within the interval (P_{q+1}, P_q) , where $q=2, 3, \dots$ the dominant contribution to the sums in Eqs. (16), (18), etc. is due to the term $\ell=q$. In $\langle \ell^2 \rangle - \langle \ell \rangle^2$, however, the main contribution is due to $\ell=q-1$ and $q+1$ because the $\ell=q$ contributions cancel out. Using this information one can find the pressure P_q^{str} within this interval for which the isothermal compressibility is minimum. The result is $P_q^{\text{str}} = (P_{q+1} + P_q)/2$ at which the contributions due to the $\ell=q-1$ and $q+1$ are exactly equal to each other. Substituting P_q^{str} back into the approximate expression for $\langle \ell^2 \rangle - \langle \ell \rangle^2$ one gets the following expression for the value of the local maximum of the diffusion coefficient static factor

$$\frac{\langle \ell \rangle^2}{\langle \ell^2 \rangle - \langle \ell \rangle^2} \Big|_{\max} = \frac{q^2}{2} e^{(1/2)\beta a \Delta P_q}, \quad (31)$$

where $\Delta P_q = P_q - P_{q+1}$, defined in Eq. (20), is the length of the pressure interval for which the coverage is equal to $1/q$ (at $T=0$, c.f. Fig. 1). The factor N is irrelevant and will be ignored from now on because it is canceled by N present in the kinetic factor.

A somewhat more detailed analysis shows that for P differing from P_q^{str} or P_{q+1} or P_q by more than $1/\beta a$ but still being between P_{q+1} and P_q , which is possible only at low enough temperatures, the P -dependence of the static factor is dominated by a single exponential. The approximate low temperature result is

$$\frac{\langle \ell \rangle^2}{\langle \ell^2 \rangle - \langle \ell \rangle^2} \propto \begin{cases} e^{\beta a (P - P_{q+1})}; & P_{q+1} < P < P_q^{\text{str}} \\ e^{\beta a (P_q - P)}; & P_q^{\text{str}} < P < P_q. \end{cases} \quad (32)$$

Consequently, for P up to P_{q+1} such that $(P_{q+1} - P_q)\beta a > 1$ the logarithm of a static factor has minima at P_2, P_3, \dots, P_{q+1} and maxima halfway between these points and is a linear function of P between the extrema. This behavior is evident in Fig. 2 in which we present the pressure dependence of the static factor (without the irrelevant factor N) for the same parameters as used in Fig. 1. The coverage dependence is shown in Fig. 3. Some comments are provided in the figure captions and we postpone further discussion until the results for the diffusion coefficient are presented.

D. The kinetic factor

It follows from Eqs. (1), (8), (9), and (30) that the kinetic factor, i.e., the jump rate diffusion coefficient, is directly related to the numerator $\mathcal{M}(k)$:

$$D_j(\theta) = N^{-1} \lim_{k \rightarrow 0} [\mathcal{M}(k)/k^2]. \quad (33)$$

In this section we will evaluate it from Eq. (10) for the lattice gas under the external pressure P . It is important to note here that evaluating the kinetic factor we use in Eq. (10) the same approximate expression, Eq. (13), for $\tilde{z}_{\{m\}}(k)$ as used to calculate the inverse of the static factor from Eq. (11). Consequently, both factors entering the expression (1) for the diffusion coefficient are evaluated from their defining exact

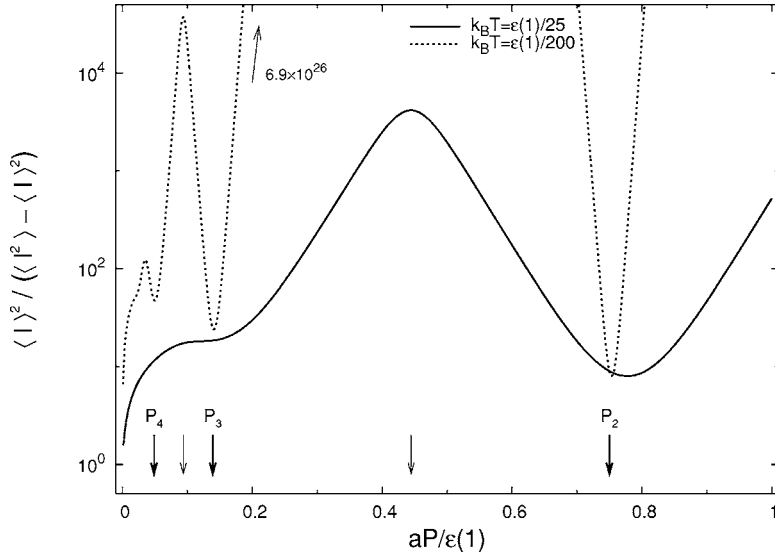


FIG. 2. The static factor, evaluated from Eq. (30) for the system with the NN-pair interaction given in Eq. (21), for “low” and “high” temperature as a function of pressure P . The arrows in the center of the intervals (P_{q+1}, P_q) indicate the pressure values P_q^{tr} at which the static factor reaches its local maximum value given in Eq. (31). The absolute maximum for the low temperature case $[\beta/\varepsilon(1)=200]$, indicated by the arrow at the top, is well beyond the scale of the graph.

expressions using the same set of approximations.

Positions of all but one particle (the one which jumps) are the same in both configurations $\{m\}$ and $\{m'\}$ in Eq. (10) while the position of the hopping particle differs by $\pm a$ between them. If the hopping particle is not the reference one then $F_{\{m\},\{m'\}}(k)=1$ and, as seen from Eq. (13), all but one term in $\tilde{e}_{\{m'\}}(k)$ is canceled by a corresponding term in $\tilde{e}_{\{m\}}(k)$. When the hopping particle is the reference particle then all exponential terms in $\tilde{e}_{\{m'\}}(k)$ differ from the corresponding exponential terms in $\tilde{e}_{\{m\}}(k)$ by a factor $\exp(\pm ika)$ which is canceled by $F_{\{m\},\{m'\}}(k)=\exp(\mp ika)$. Consequently, the result is the same for any hopping particle,

$$|F_{\{m\},\{m'\}}(k)\tilde{e}_{\{m'\}}^*(k) - \tilde{e}_{\{m\}}^*(k)|^2 = 4 \sin^2\left(\frac{ka}{2}\right) \quad (34)$$

and, in the $k \rightarrow 0$ limit, we get from Eq. (10)

$$\mathcal{M}(k; L, T, N) = (ka)^2 \sum_{\{m\}, \{m'\}}^{\text{no rep}} P_{\{m'\}}^{\text{eq}} W_{\{m\}, \{m'\}}. \quad (35)$$

Further progress requires a closer look at the hopping rates.

The sum over configuration pairs $\{m\}, \{m'\}$ in Eq. (35) may be replaced with the summation in which we fix the initial configuration $\{m'\}$, evaluate and add together all contributions resulting from considering each particle in it, one at a time, to be the hopping one, repeating the process for all possible configurations $\{m'\}$, and adding the results. To avoid counting any pair of configurations $\{m\}, \{m'\}$ twice we allow in the above procedure only jumps in one, clockwise, for example, direction. In other words, given configuration $\{m'\}$ and a given hopping particle contribute at most one term (none, if the site to the right of the hopping particle is already occupied in $\{m'\}$). Focus now attention on a given hopping particle in $\{m'\}$. Assume that its distance (in units of a) from its nearest neighbor in the counterclockwise direction (i.e., to its left) is l while the distance in the clockwise direction (to its right) is r , where l and r are integers. In the final configuration $\{m\}$ the corresponding distances of the hopping particle are $r-1$ and $l+1$. The equilibrium probability $P_{\{m'\}}^{\text{eq}}$ is a complicated function of $\ell_1, \ell_2, \dots, l, r, \dots, \ell_{N-1}, \ell_N$ which are the lengths of the subsequent NN-pairs (N in total) in this configuration. Among them, the particular lengths l and r

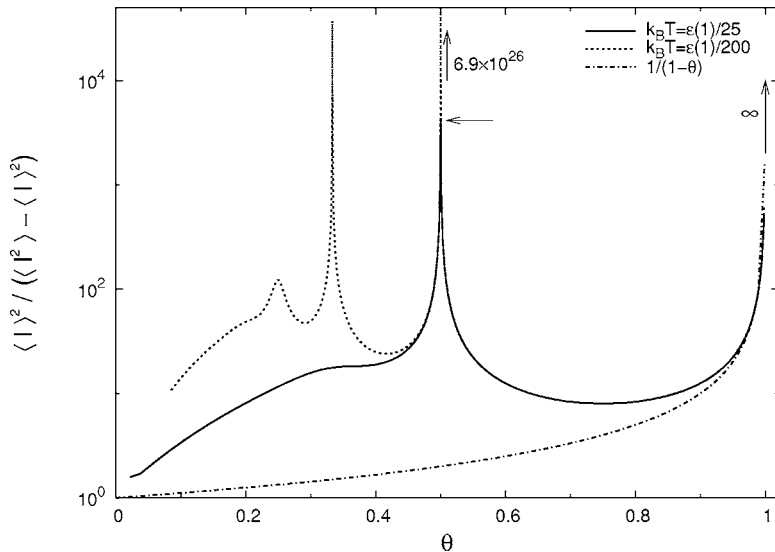


FIG. 3. The same as in Fig. 2 but as a function of coverage. For full coverage the static factor is infinite because the system is ideally rigid. The peaks at $\theta=1/q$ are generated by the points within the pressure interval (P_{q+1}, P_q) in Fig. 2. The horizontal arrow indicates the height of the $\theta=1/2$ peak for $\beta/\varepsilon(1)=25$ (cf. the central peak in Fig. 2). The static factor for the noninteracting system, cf. Eqs. (30) and (40c), is shown for comparison.

appear at two adjacent positions in the list (l preceding r). The complication is, as before, due to the finite length L of the entire system. Replacing the system with fixed L with a system under an external pressure P results in replacing this combined probability with a product $p_{\ell_1} p_{\ell_2} \dots p_l p_r \dots p_{\ell_N}$ of the probabilities defined in Eq. (14).

We assume now that the jump rate of the process in which the lengths of two adjacent NN-pairs, l and r , change into $l+1$ and $r-1$, respectively, depend only on these two lengths but does not depend on the lengths of all $N-2$ remaining NN-pairs. This is a reasonable assumption for the system in which the jumping particle interacts only with the first neighbors to its left and right. We denote this rate $W_{l+1,r-1}^{l,r}$. It is related to the rate of the return jump in the counterclockwise direction through the detailed balance condition

$$W_{l+1,r-1}^{l,r} p_l p_r = W_{l,r}^{l+1,r-1} p_{l+1} p_{r-1}. \quad (36)$$

With that, a contribution due to a particular initial configuration $\{m'\}$ and a particular hopping particle in it is $W_{l+1,r-1}^{l,r} p_{\ell_1} p_{\ell_2} \dots p_l p_r \dots p_{\ell_N}$. Summation over the initial configurations involve $N-2$ summations over all ℓ_j 's from 0 to ∞ , which add up to 1^{N-2} because p_{ℓ} 's are normalized. The hopping particle can be any of the N particles in the system, summing over this possibility results in the overall factor N . Finally, we have summation over the lengths l and r starting from 1 and 2, respectively. The final result is

$$\mathcal{M}(k; P, T, N) = (ka)^2 N \sum_{l=1}^{\infty} \sum_{r=2}^{\infty} W_{l+1,r-1}^{l,r} p_l(P, T) p_r(P, T). \quad (37)$$

This general expression allows investigating diffusion in systems with different kinetics and with different interaction models. The only restriction is NN approximation.³⁵ Although the summation in Eq. (37) runs only over the jumps in the clockwise direction a simple transformation using the detailed balance can convert the sum to run exclusively over the counterclockwise jumps.

III. PARTICULAR INTERACTION CASES

Let the energy of an isolated particle adsorbed at an arbitrary lattice site be E_A^0 . The sites are separated by potential energy barriers at which the potential energy of a particle is E_B^0 , higher than E_A^0 . With no particle-particle interactions a particle must be supplied an energy $E_B^0 - E_A^0$ from a thermal bath of the substrate so the isolated particle jump rate is

$$W^0 = \nu^0 e^{-\beta(E_B^0 - E_A^0)}, \quad (38)$$

where ν^0 is referred to as an attempt frequency and $\beta = 1/k_B T$. For the many-particle system the mutual interactions modify both the thermodynamic properties of the system as well as the kinetic ones. We want to analyze the resulting coverage dependence of the chemical diffusion coefficient as well as that of the kinetic and static factors, defined in Secs. II C and II D. It is worthwhile to start with the simplest interaction models in order to confront the results with the results already known.

A. Noninteracting lattice gas

With no interactions $\varepsilon(\ell) = 0$ for all ℓ 's and $W_{l+1,r-1}^{l,r} = W^0$. The only restriction is that no two particles can occupy the same site. The calculation of Z_1 and \mathcal{M} reduces to summations of $\exp(-\beta a P \ell)$ over ℓ . Defining an auxiliary parameter s ,

$$s = e^{-\beta a P}, \quad (39)$$

and using Eqs. (14)–(17) and (30) we get

$$Z_1(P, T) = \frac{s}{1-s}, \quad (40a)$$

$$\langle \ell \rangle \equiv \frac{1}{\theta} = \frac{1}{1-s}, \quad (40b)$$

$$\mathcal{N}(k=0; P, T, N) = Ns = N(1-\theta), \quad (40c)$$

while the kinetic factor (the numerator), from Eq. (37), is

$$\mathcal{M}(k; P, T, N) = (ka)^2 N W_0 s = (ka)^2 N W^0 (1-\theta). \quad (41)$$

Equation (40b) is the equation of state relating pressure coverage and temperature. Upon combining these results the factors $1-\theta$ in Eqs. (40b) and (41) cancel out yielding the chemical diffusion coefficient

$$D(\theta) = W^0 a^2, \quad (42)$$

which does not depend on coverage. This well-known result was derived repeatedly using various approaches.^{8,24,37}

B. Short-range interactions

In this case the particles interact only when they occupy neighboring sites. Following Ref. 25 we assume

$$\varepsilon(\ell) = \begin{cases} J & \text{for } \ell = 1 \\ 0 & \text{for } \ell \geq 2, \end{cases} \quad (43)$$

with repulsive interactions between particles at nearest-neighbor sites for $J > 0$ and attractive ones for $J < 0$. The kinetics is defined by specifying four hopping rates

$$W_{l+1,r-1}^{l,r} = \begin{cases} W^0; & l \geq 2, r \geq 3; \quad \dots \circ \bullet \rightarrow \circ \circ \dots \\ \Gamma; & l = 1, r \geq 3; \quad \dots \bullet \bullet \rightarrow \circ \circ \dots \\ R; & l \geq 2, r = 2; \quad \dots \circ \bullet \rightarrow \circ \bullet \dots \\ T; & l = 1, r = 2; \quad \dots \bullet \bullet \rightarrow \circ \bullet \dots \end{cases} \quad (44)$$

An arrow in Eq. (44) identifies a particular atomic jump taking an atom denoted by a \bullet to an empty site \circ immediately to the right of the arrow. The sites to the left of the initial and to the right of the target site may be either vacant (\circ) or occupied (\bullet)—the hopping rate depends on these occupation states. A string of more distant sites whose occupation does not affect the hopping rate and which can either be occupied or empty is represented by \dots . With the interaction parameter

$$p = e^{\beta J}, \quad (45)$$

the detailed balance condition for the rates R and Γ , corresponding to jumps in opposite directions, reads

$$\Gamma = pR. \quad (46)$$

Also in this case all quantities of interest can be obtained by calculating sums of $\exp(-\beta a P \ell)$ over ℓ starting from 1, 2, or 3. We get

$$Z_1(P, T) = s \left(\frac{1}{p} + \frac{s}{1-s} \right), \quad (47a)$$

$$\langle \ell \rangle \equiv \frac{1}{\theta} = 1 + \frac{ps}{(1-s)[1+(p-1)s]}, \quad (47b)$$

$$\mathcal{N}(k=0; T, P, N) = \frac{Nps[1+(p-1)s^2]}{[p+(1-p)(1-s)^2]^2}, \quad (47c)$$

where Eq. (47b) is the equation of state allowing one to determine the θ dependence of s (i.e., of P). The kinetic factor is as easy:

$$\mathcal{M}(k; P, T, N) = (ka)^2 \frac{Ns^3}{[Z_1(P, T)]^2} \times \left\{ W^0 \left(\frac{s}{1-s} \right)^2 + 2R \frac{s}{1-s} + \frac{T}{p} \right\}. \quad (48)$$

Combining these results according to Eqs. (8) and (9) we get the collective diffusion coefficient

$$D[s(\theta)] = a^2 \frac{ps^2[p+(1-p)(1-s)^2]^2}{[1+(p-1)s]^2[1+(p-1)s^2]} \times \left\{ W^0 + 2R \frac{1-s}{s} + \frac{T}{p} \left(\frac{1-s}{s} \right)^2 \right\}, \quad (49)$$

which agrees with the result obtained in a more complicated way in Ref. 25 where numerical implications and a detailed comparison with results of numerical simulations are presented (s is denoted r there). Here, we note only that the result in Eq. (49) exhibits the particle-hole symmetry: it returns the same function of θ upon the exchanges $W^0 \leftrightarrow T$ and $\theta \leftrightarrow (1-\theta)$. Also, with $W^0 = T = R = \Gamma$ and, consequently, with $p=1$, all results from Sec. III A are reproduced.

C. Long-range interactions

Here, we assume that the particles interact at an arbitrary distance as long as there are no particles between them. Static properties of such a system, investigated in Ref. 35, have been summarized in the concluding paragraph of Sec. II B. Although many qualitative properties of the system do not depend on the particular functional form of the interparticle interaction as long as it is repulsive and, as a function of ℓ —considered as a continuous variable—is a convex function vanishing faster than ℓ^{-1} , we will be illustrating our results for the long-range interaction energy given in Eq. (21).

To specify the kinetics we propose to investigate three distinct models with different interactions between the activated hopping particle, instantaneously at a bridge site between its initial and the target adsorption site, and other adsorbed particles. The models are defined in three separate

sections, Secs. III C 1–III C 3, to follow. Each model leads to different expression for the kinetic factor $\mathcal{M}(k; P, T, N)$, cf. Eqs. (55), (58), and (61) to follow, and the full diffusion coefficient is obtained by multiplying either of them by the same static factor $1/\mathcal{N}(k=0; P, T, N)$ discussed in Sec. II C and displayed in Figs. 2 and 3.

1. Interacting activated particle: Averaged bridge-site potential energy

We consider first a class of kinetic models obtained by relating the height of the potential barrier which a hopping particle must surmount while hopping between adjacent adsorption sites to the potential energies of the particle at either its initial or target adsorption site or both. We consider the particle hopping from the adsorption site specified by a pair of integers (l, r) (i.e., with the nearest-neighbor adsorbed particles being at a distance al and ar , respectively, to its left and right) to a neighboring site (l', r') . Of course, $l+r=l'+r'$ is the distance between the neighbors themselves, and $l'-l=r-r'=\pm 1$ with the upper/lower sign pertaining to the jump in the clockwise/counterclockwise direction. The potential energy at the initial adsorption site is

$$E_A = E_A^0 + \varepsilon(l) + \varepsilon(r), \quad (50)$$

and a similar expression holds for the potential energy at the target site. The hopping rate can be written as

$$W_{l',r'}^{l,r} = W^0 e^{-\beta[\Delta_{l',r'}^{l,r} - \varepsilon(l) - \varepsilon(r)]}, \quad (51)$$

where $\Delta_{l',r'}^{l,r}$ is the amount by which the potential energy of the hopping particle at a bridge site between its initial and the final position is modified by interactions with the neighbors at each its side.

The model of kinetics which we consider is best defined by denoting, for simplicity, $E = \varepsilon(l) + \varepsilon(r)$, $E' = \varepsilon(l') + \varepsilon(r')$ and assuming that the potential energy correction at the barrier site, $\Delta_{l',r'}^{l,r}$, is fully determined by these energy corrections at both involved adsorption sites, i.e., $\Delta_{l',r'}^{l,r} = \Delta(E', E)$. One possibility is to assume that the potential energy at the bridge site is modified due to interactions by exactly the same amount as is the potential energy at that of the two adsorption sites involved which, after modifications, remains deeper of the two. Therefore the barrier height correction and the resulting from Eq. (51) hopping rate are

$$\Delta(E', E) = \min(E', E),$$

$$W_{l',r'}^{l,r} = W^0 \begin{cases} e^{-\beta(E'-E)} & \text{for } E' \leq E \\ 1 & \text{for } E' \geq E. \end{cases} \quad (52)$$

One can verify that the rates satisfy the detailed balance condition. For repulsive interactions the hopping rates are either the same as or faster than that for an isolated particle (W^0).

In the other extreme case the potential energy at the bridge site is modified by the same amount as that at that adsorption site which remains shallower of the two. In this case

$$\Delta(E', E) = \max(E', E),$$

$$W_{l',r'}^{l,r} = W_0 \begin{cases} 1 & \text{for } E' \leq E \\ e^{-\beta(E'-E)} & \text{for } E' \geq E. \end{cases} \quad (53)$$

Here, the repulsive interactions slow down the rates or leave them unchanged in comparison to W^0 . This does not imply the overall slowing down of diffusion [or speeding it up for the model in Eq. (52)] by the interactions because, as we have already seen, the static factor also depends strongly on interactions.

We wish to examine a continuum of models of kinetics between the two extremes listed above. In the simplest case we assume that $\Delta(E', E)$ is a weighted average (with weight controlled by a continuous parameter γ) of the barrier corrections from Eqs. (52) and (53). The barrier height correction and the resulting hopping rate are

$$\begin{aligned} \Delta(E', E) &= \frac{1}{2} \{ (1 + \gamma) \min(E, E') + (1 - \gamma) \max(E, E') \} \\ &= \frac{1}{2} \{ E + E' - \gamma |E - E'| \}, \end{aligned}$$

$$\begin{aligned} W_{l',r'}^{l,r} &= W_0 e^{-\beta(E'-E)/2} e^{\gamma\beta(E'-E)/2} \\ &= W_0 e^{-\beta[\epsilon(l') + \epsilon(r') - \epsilon(l) - \epsilon(r)]/2} \\ &\quad \times e^{\gamma\beta[\epsilon(l') + \epsilon(r') - \epsilon(l) - \epsilon(r)]/2}. \end{aligned} \quad (54)$$

For $\gamma = +1$ and $\gamma = -1$ we obtain the models of kinetics from Eqs. (52) and (53), respectively. For $\gamma = 0$ the interaction induced barrier height correction is an arithmetical average of the potential energy corrections at both adsorption sites involved.

Using the above rate for $l' = l + 1$ and $r' = r - 1$ in Eq. (37) yields the following expression for the kinetic factor

$$\begin{aligned} \mathcal{M}(k; P, T, N) &= (ka)^2 \frac{NW^0}{[Z_1(P, T)]^2} e^{-\beta a P} \\ &\quad \times \left\{ \sum_{\ell=1}^{\infty} e^{-\beta[\epsilon(\ell) + \epsilon(\ell+1) + 2a\ell P]} \right. \\ &\quad + 2 \sum_{\ell=2}^{\infty} e^{-\beta[(1-\gamma)/2\epsilon(\ell+1) + (1+\gamma)/2\epsilon(\ell) + a\ell P]} \\ &\quad \left. \times \sum_{\ell'=1}^{\ell-1} e^{-\beta[(1-\gamma)/2\epsilon(\ell') + (1+\gamma)/2\epsilon(\ell'+1) + a\ell' P]} \right\}. \end{aligned} \quad (55)$$

Note that the single sum together with the preceding term $e^{-\beta a P}$ can be written as $\sum_{\ell=1}^{\infty} p_{\ell}(P, T) p_{\ell+1}(P, T)$, where $p_{\ell}(P, T)$ is defined in Eq. (14) probability of a pair of length $a\ell$. Only for $\gamma = \pm 1$ the double sums contribution can be also written in terms of products of such probabilities. The results are

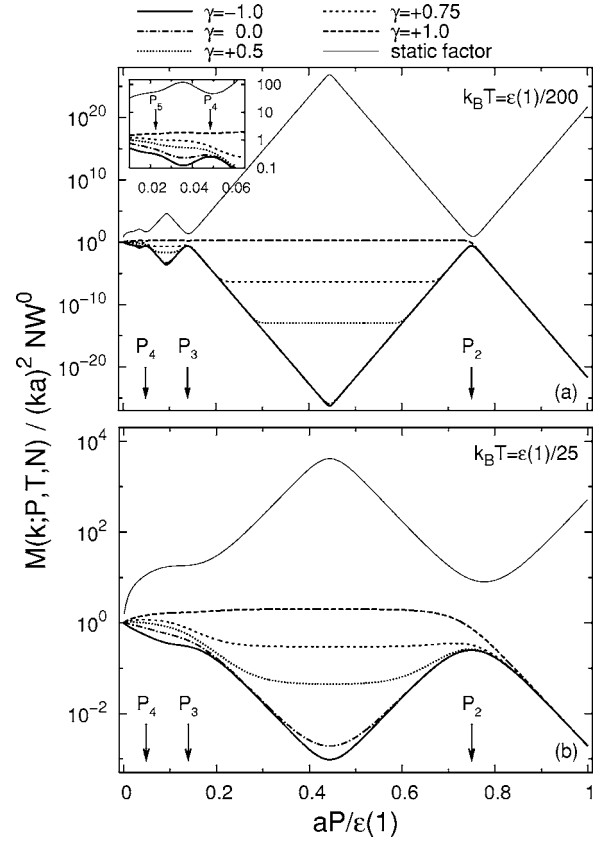


FIG. 4. Pressure dependence of the diffusion coefficient kinetic factor (the numerator) defined in Eq. (55) (averaged bridge-site energy model) for the interaction energy in Eq. (21) for low (a), and high (b) temperatures for several values of the control parameter γ . The inset in panel (a): a magnified view around pressures P_4 and P_5 . The static factor from Fig. 2 is also plotted.

$$\begin{aligned} \left. \frac{\mathcal{M}(k; P, T, N)}{(ka)^2 NW^0} \right|_{\gamma=-1} &= \sum_{\ell=1}^{\infty} p_{\ell} p_{\ell+1} + 2 \sum_{\ell=2}^{\infty} \sum_{\ell'=1}^{\ell-1} p_{\ell+1} p_{\ell'} \\ &\approx p_q (p_{q-1} + p_{q+1}), \end{aligned} \quad (56a)$$

$$\left. \frac{\mathcal{M}(k; P, T, N)}{(ka)^2 NW^0} \right|_{\gamma=+1} = \sum_{\ell=1}^{\infty} p_{\ell} p_{\ell+1} + 2 \sum_{\ell=2}^{\infty} \sum_{\ell'=1}^{\ell-1} p_{\ell} p_{\ell'+1} \approx 2p_q, \quad (56b)$$

where the approximate expressions are valid for P between P_{q+1} and P_q ($q=2, 3, 4, \dots$) but further away from the interval ends than $1/\beta a$ [P_q 's are defined in Eq. (19)]. Within this interval $p_q(P, T) \approx 1$ so the kinetic factor is approximately independent of P for $\gamma = +1$. For $\gamma = -1$ only one of the two terms dominates in the sum $p_{q-1}(P, T) + p_{q+1}(P, T)$ so the kinetic factor exponentially decreases with P for $P < P_q^{\text{xtir}}$ and increases above P_q^{xtir} , i.e., its pressure dependence is exactly inverse to that of the static factor shown in Eq. (32). This will be seen explicitly later on in Sec. IV—in Fig. 4, in particular. Consequently varying models of kinetics by changing the control parameter γ we expect, at low temperatures at least, a continuous transition from almost perfect

compensation between the kinetic and the static factor, resulting in the diffusion coefficient which depends very weakly on P and θ (case of $\gamma=-1$) to no compensation at all, resulting in the diffusion coefficient following, as a function of P or θ , variations of the static factor (case of $\gamma=+1$).

2. Noninteracting activated particle

We turn our attention to a model of kinetics most frequently used in numerical simulations. Here, only the energy of the nonactivated hopping particle at its adsorption sites is modified by interparticle interactions while the energy at a bridge site between the initial and the target adsorption site remains the same as for isolated particles. This results in the hopping rate given in Eq. (51) with $\Delta_{l,r}^{l',r'}=0$

$$W_{l',r'}^{l,r} = W^0 e^{\beta[\varepsilon(l)+\varepsilon(r)]}, \quad (57)$$

which are faster than W^0 . This should lead to more efficient diffusion with increasing coverage.

Using the rates given in Eq. (57) in Eq. (37) the diffusion coefficient kinetic factor becomes

$$\mathcal{M}(k; P, T, N) = (ka)^2 \frac{NW^0}{[Z_1(P, T)]^2 (1-s)^2}, \quad (58)$$

where s is given in Eq. (39) and $Z_1(P, T)$ must be evaluated from Eq. (16) using particular interaction function $\varepsilon(l)$. The diffusion coefficient is obtained using Eqs. (58) and (30) in Eqs. (8) and (9). All statistical sums, e.g., Eq. (16), must be evaluated numerically.

Two observations can be made even before numerical results are presented: (i) At full coverage all hopping events effectively occur for $l=1$ and $r=2$ so, at a microscopic level, diffusion is due to a random walk of holes hopping between the adjacent sites at a rate $W^0 \exp[5\beta\varepsilon(1)/4]$ [for $\varepsilon(l)$ given in Eq. (21)]. Therefore the diffusion coefficient at $\theta=1$ is expected to be $\exp[5\beta\varepsilon(1)/4]$ times larger than that at $\theta=0$. Obviously, the $1/(1-\theta)$ divergence of the static factor in the $\theta \rightarrow 1$ limit (cf. Fig. 3) has to be exactly compensated by the $1-\theta$ dependence of the kinetic factor. (ii) The kinetic factor in Eq. (58) depends on the particular form of $\varepsilon(l)$ only through $Z_1(P, T)$. Consequently, the result in Eq. (58) should also be valid in the case of short-range interactions, defined in Eq. (43), provided we select hopping rates corresponding to the interaction-independent barrier heights. This means $R=W^0$ and $T=\Gamma=pW^0$ as easily seen by examining each case listed in Eq. (44) and by using Eq. (46). Indeed, with these substitutions, Eq. (48) for the kinetic factor corresponding to the short-range interaction case reduces to the one given in Eq. (58). The appropriate $Z_1(P, T)$ is given in Eq. (47a) in this case.

3. Interacting activated particle: Centered bridge-site

Obviously, there is no compelling reason for the potential energy of the activated particle (at a barrier site) to be independent of the interparticle interactions. Apart from a model proposed in Sec. III C 1 one of the simplest models taking into account such interactions is obtained by realizing that the particle at the adsorption site (l, r) hopping to the site

$(l+1, r-1)$ surmounts a potential energy barrier at a bridge site situated, approximately, at a distance $l+\frac{1}{2}$ and $r-\frac{1}{2}$ from its nearest left and right adsorbed particle, respectively, and by evaluating the bridge site potential energy using $\varepsilon(l)$ generalized to half-integer arguments. Consequently, in analogy to Eq. (50), the potential energy correction at the bridge site between (l, r) and $(l+1, r-1)$ adsorption sites is

$$\Delta_{l+1, r-1}^{l, r} = \varepsilon\left(l + \frac{1}{2}\right) + \varepsilon\left(r - \frac{1}{2}\right), \quad (59)$$

which, used in Eq. (51), leads to the following hopping rate for the clockwise jumps:

$$W_{l+1, r-1}^{l, r} \equiv \nu^0 e^{-\beta(E_B - E_A)} = W^0 e^{-\beta[\varepsilon(l+1/2) + \varepsilon(r-1/2) - \varepsilon(l) - \varepsilon(r)]}. \quad (60)$$

It is easy to check that a similar expression for the counterclockwise jumps with $\Delta_{l-1, r+1}^{l, r} = \varepsilon(l-\frac{1}{2}) + \varepsilon(r+\frac{1}{2})$ is consistent with the one obtained from Eq. (60) using the detailed balance condition and that for $l=r$ the jump rates from the site $(l, r=l)$ in the clockwise and the counterclockwise directions are the same.

Using Eq. (60) in Eq. (37) yields the kinetic factor

$$\mathcal{M}(k; P, T, N) = (ka)^2 \frac{NW^0}{[Z_1(P, T)]^2} \left[\sum_{\ell=1}^{\infty} e^{-\beta\tilde{\varepsilon}(\ell+1/2)} \right]^2, \quad (61)$$

in which the definition of $\tilde{\varepsilon}$ in Eq. (16) is used. Similarly like in $Z_1(P, T)$ in Eq. (16) the main contribution to the sum over ℓ in Eq. (61) comes from one or at most two terms for low enough temperatures but, for a given value of P , they may correspond to different ℓ than terms most significant in Z_1 . In general, the sum has to be evaluated numerically.

IV. NUMERICAL RESULTS AND DISCUSSION

Presenting the results we want to pay particular attention to the question: how much of the coverage dependence of the static factor [which is inversely proportional to the isothermal compressibility—cf. Eq. (30)] is evident in the concentration dependence of the collective diffusion coefficient. For the noninteracting system, for example [cf. Sec. III A], the coverage dependence of the static factor proportional to $1/(1-\theta)$ is exactly compensated for by the $1-\theta$ dependence of the kinetic factor. This results in the coverage independent collective diffusion coefficient. The static factor does not depend on details of kinetics of particle migration—it depends only on interparticle interactions (and the substrate—particle interactions) for particles adsorbed at the regular adsorption sites. The kinetic factor depends on these interactions too but it depends also on interactions between a migrating particle in an activated state and the rest of the system. In this work we have proposed several models of kinetics possible for a system with an equation of state leading to a static factor exhibiting sharp peaks at certain isolated values of coverage (at which the system has abnormally low compressibility). Superficially, one might expect that such singular behavior

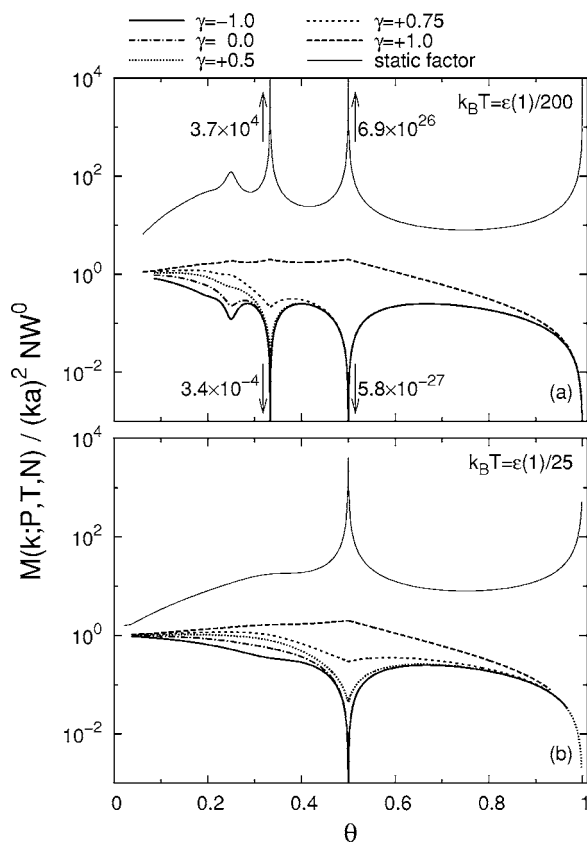


FIG. 5. The same as in Fig. 4 but as a function of coverage. The static factor is the same as in Fig. 3. Sharp minima of the kinetic factor occur for models with lower γ at $\theta = 1/q$, $q = 2, 3, \dots$ at which the static factor has sharp maxima. Peak values are listed in cases where they are outside the plotted range.

would be difficult to compensate for in a kinetic factor and, consequently, the collective diffusion coefficient would also increase sharply at these values of coverage.

In what follows we will examine the coverage dependence of the kinetic factor and the diffusion coefficient for the system with long-range interactions and present all numerical results for the interaction energy given in Eq. (21). To understand the coverage dependence of all quantities involved here it is advantageous to examine, at the same time, their pressure dependence. We have seen already for the static factor that its coverage dependence in Fig. 3 can be easily rationalized by combining its easily understandable pressure dependence (Fig. 2) with the shape of the isotherms of the system, shown in Fig. 1. The systems with short-range interactions, described in Sec. III B, were already analyzed, albeit from a different perspective, in Ref. 25.

We start with the averaged bridge-site potential energy model of kinetics (Sec. III C 1) in which the control parameter γ allows one to tune the dependence of the hopping barrier height on the initial and the target adsorption site potential energy of a hopping particle. The kinetic factor is plotted in Fig. 4 as a function of pressure and in Fig. 5 as a function of coverage for two temperatures used already in Figs. 1 and 2 for several values of the parameter γ . The static factor, also shown in these figures, is the same as in Figs. 2 and 3. Concentrating at lower temperature [Fig. 4(a)] we

note that for $P > P_2$ for which, according to Fig. 1, the coverage is $\theta = 1$, the kinetic factors for all values of the control parameter γ decrease exponentially with pressure at the exact same rate as the static factor increases. We have a perfect compensation here. We have seen in Fig. 3 that the static factor is proportional to $1/(1-\theta)$ for $\theta \rightarrow 1$ and the behavior observed in Fig. 4 indicates that the kinetic factor should, therefore, be proportional to $1-\theta$ in this limit.

For $P < P_2$ the kinetic factor depends on γ , i.e., it depends on details of kinetics. At the end Sec. III C 1 we have argued that for kinetics corresponding to $\gamma = -1$, pressure and coverage dependence of the kinetic factor should almost perfectly compensate those of the static factor while for $\gamma = +1$ there should be no compensation at all. This is, indeed, the case in Fig. 4(a) where the kinetic factor for all negative values of γ is practically identical in the interval of $P > P_4$. In the logarithmic plots in Figs. 4(a) and 5(a) the kinetic factor looks almost like a mirror image of the static factor indicating an almost perfect compensation in this interval. For $P < P_4$ the arguments used to derive the approximate result in Eq. (56a) no longer applies because the length of the intervals (P_5, P_4) , $(P_6, P_5), \dots$, become first comparable and then smaller than $1/\beta a$ even at these low temperatures [cf. inset in Fig. 4(a)]. For $\gamma = +1$ the opposite is true. Here, in agreement with Eq. (56b) and the discussion below it, the kinetic factor is almost independent of P for pressures up to P_2 . In Fig. 5 (θ dependence) the $\gamma = +1$ line is almost featureless and only when $\theta \rightarrow 1$ it joins the $1-\theta$ behavior together with lines corresponding to other γ 's. We have no compensation here and the P and θ dependence of the diffusion coefficient should follow those of the static factor. It is, therefore, easy to understand the behavior of the diffusion coefficient observed in Figs. 6(a) and 7(a). The diffusion coefficient for $\gamma = +1$ closely follows the lines representing the static factor (except for $P > P_2$) with sharp peaks at $\theta = 1/2$ and $1/3$ and a broader maximum around $\theta = 1/4$ [cf., Fig. 7(a)] while no singular feature of the static factor survives in diffusion for $\gamma = -1$. In the latter case the diffusion coefficient reaches around $\theta = 0.2$ a broad maximum about an order magnitude above its low coverage value $W^0 a^2$ and then decreases slowly back to $W^0 a^2$. For all $\gamma < 0$ the P and θ dependence of the kinetic factor (and, consequently, the diffusion coefficient) is almost identical to that for $\gamma = -1$, the differences occur only for $P < P_3$. For $\gamma > 0$ the limiting $\gamma = +1$ behavior is reached gradually: while the kinetic factor still compensates the P dependence of the static factor close to $P = P_2, P_3, \dots$ it becomes independent of P around $P_2^{\text{tr}}, P_3^{\text{tr}}$, etc. over intervals of P which grow with increasing γ . This is evident in Fig. 4(a) in a progression of lines corresponding to $\gamma = +0.5, +0.75$, and $+1$. The resulting diffusion coefficient dependence on P and θ can be seen in Figs. 6(a) and 7(a). In particular peaks at $\theta = 1/2, 1/3$, and $1/4$ become smaller with increasing γ until for $\gamma = +1$ they disappear entirely.

All the features seen in Figs. 4(a)–7(a) at low temperatures are also present in panels (b) of the figures, corresponding to a higher temperature. With $1/\beta a$ being almost an order of magnitude higher than in panels (a) of the figures, all the sharp features in the P dependence are rounded off and the resulting diffusion coefficient has only one sharp peak at $\theta = 1/2$ [Fig. 7(b)] which, of course, disappears for the model of kinetics corresponding to $\gamma = +1$.

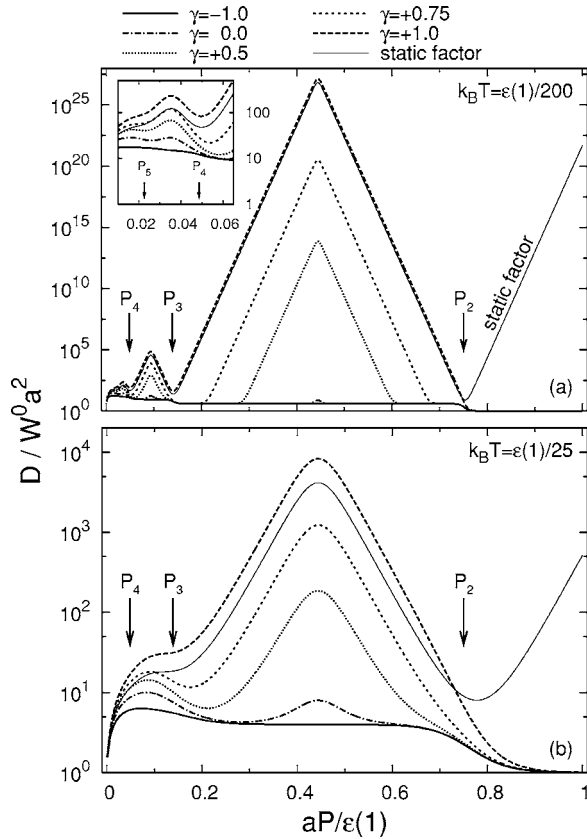


FIG. 6. Pressure dependence of the chemical diffusion coefficient—a product of the static factor (shown also here in this plot) and the kinetic factors presented in Fig. 4. The values of temperature and those of the control parameter γ are the same as in Fig. 4.

A characteristic feature of all models of kinetics discussed above (and defined in Sec. III C 1) is that at the full coverage the hopping rate of an isolated hole is the same as the hopping rate of an isolated particle at $\theta=0$. Consequently, the diffusion coefficient is equal to $W^0 a^2$ in both these limits. This is not the case for two remaining models of kinetics investigated here: noninteracting activated particle model of Sec. III C 2 and the centered bridge-site model of Sec. III C 3. For full coverage all hopping events (in the presence of a single hole) occur for $l=1$ and $r=2$ (clockwise direction) resulting in an isolated hole hopping rate which is larger than W^0 by a factor of $\exp[5\beta\epsilon(1)/4]$ for the former [cf. Eq. (57)] and of $\exp[13\beta\epsilon(1)/36]$ for the latter model [cf., Eq. (60)]. Consequently, the diffusion coefficient is expected to increase in both models by these factors (i.e., by many orders of magnitude) when the coverage increases from 0 to 1. This is seen in Figs. 8 and 9. The static factor (the same as in Figs. 2 and 3, respectively), the kinetic factor, and the collective diffusion coefficient are plotted in Fig. 8 as functions of P for the activated state interaction model of Sec. III C 2 [noninteracting activated particle—curves (a)] and that of Sec. III C 3 [centered bridge-site—curves (b)]. The coverage dependence of the same quantities is plotted in Fig. 9. The higher of the two temperatures considered so far is used in the plots. As seen in Fig. 8, the compensation between the

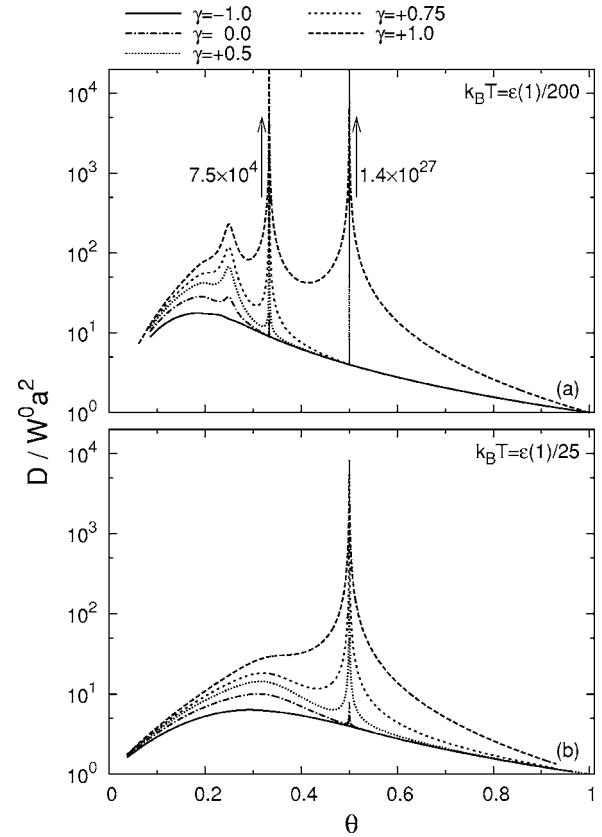


FIG. 7. The same as in Fig. 6 but as a function of coverage. The diffusion coefficient peaks at coverages $\theta=1/q$, $q=2,3,\dots$ for lower values of the control parameter γ . The peak values are given when they are outside of the plotted range.

static and the kinetic factor is more complicated than in cases discussed so far. We have the “usual” compensation for $P > P_2$. There is also compensation below P_2 but only down to P_2^{str} [a middle-point between P_3 and P_2 , cf., above Eq. (31)] below which the kinetic and the static factor increase exponentially with P at the same rate leading to even faster increase of the diffusion coefficient. Below P_2 all sharp features are masked by the thermal effect of high temperature. Consequently, the diffusion coefficient raises rapidly with P until $P=P_2^{\text{str}}$ and then varies slowly because of an almost perfect compensation. The initial increase is particularly rapid in the noninteracting activated particle model. Translating this behavior to the coverage dependence (Fig. 9) we observe a rapid increase of the diffusion coefficient with θ followed by a sharp, almost discontinuous increase at $\theta=1/2$ (its origin is similar to that of the peak at $\theta=1/2$ in the models considered before) after which the diffusion remains almost constant. For the centered bridge-site model the entire increase of the diffusion from its value at $\theta=0$ to that at $\theta=1$ occurs almost discontinuously around $\theta=1/2$.

V. COMMENTS ON DEVIL'S STAIRCASE SYSTEM

As already mentioned in Sec. I, this work is partially motivated by experiments^{20,21} indicating that Pb adsorbed at the Si(111) surface provides an example of the devil's staircase

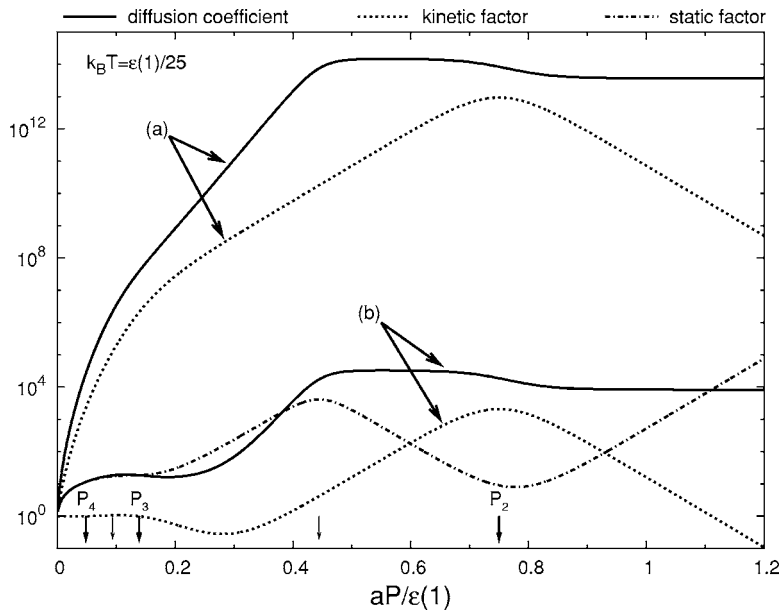


FIG. 8. Pressure dependence of the static factor (same as in Fig. 2), the kinetic factor, and the resulting diffusion coefficient for: (a) the non-interacting activated particle model of Sec. III C 2 [Eq. (58)] and (b) the centered bridge-site model of Sec. III C 3 [Eq. (61)] for the higher of the two temperatures used in previous figures.

system with a high degree of self-organization driven by long range repulsive interactions between the adsorbed atoms. Fast transformations from one structural phase to another one upon minute changes in coverage, which occur at low temperatures without any annealing of the system and which require reorganization of the adsorbate over macroscopic regions, suggest that the diffusion coefficient, as a function of coverage, has sharp maxima at slightly differing from each other coverages equal to irreducible ratios of small integers, $\theta = m/n$.

Equilibrium properties of the Ising Model devil's staircase system have been investigated in the past³² and in the context of the present work it is isomorphic with a one-dimensional lattice gas in which any particle, at a lattice position ℓ_i say, interacts with any (not only the nearest) particle at ℓ_j . The interaction must be repulsive and its energy $\varepsilon(\ell_i - \ell_j)$ must decline faster than $1/|\ell_i - \ell_j|$ and be a convex function of its

argument. The isotherms for this system, e.g., plots of coverage θ vs chemical potential μ have, at low temperatures, a fractal devil's staircase character with an infinite number of plateaus at rational number coverages $\theta = m/n$. The interval of μ over which the phase corresponding to $\theta = m/n$ (with $m < n$) is stable, i.e., the width of the $\theta = m/n$ plateau, is³²

$$\Delta\mu\left(\frac{m}{n}\right) = n \sum_{s=1}^{\infty} s [\varepsilon(ns - 1) - 2\varepsilon(ns) + \varepsilon(ns + 1)]. \quad (62)$$

It does not depend on m and the stability decreases with increasing n [due to decrease of $\varepsilon(\ell)$ with increasing ℓ]. In the order of decreasing stability we have: the most stable phase corresponding to $\theta = 1/2$; two equally stable phases with $\theta = 1/3$ and $2/3$; the next two with $\theta = 1/4$ and $3/4$; followed by four equally stable ones with $\theta = 1/5$, $2/5$, $3/5$, and $4/5$, and so on. Note the similarity between Eq. (62) and

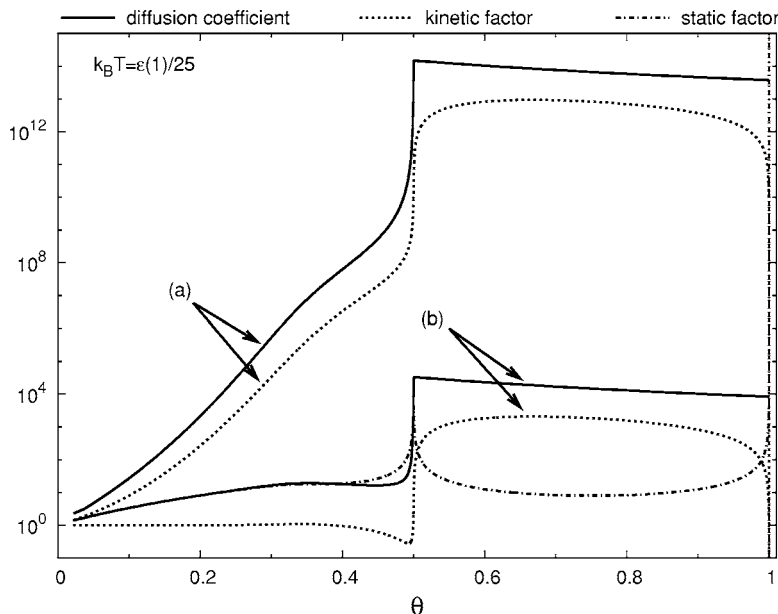


FIG. 9. The same as in Fig. 8 but as a function of coverage. The static factor is the same as in Fig. 3. (a)—the non-interacting activated particle model of Sec. III C 2 [Eq. (58)] and (b)—the centered bridge-site model of Sec. III C 3 [Eq. (61)]

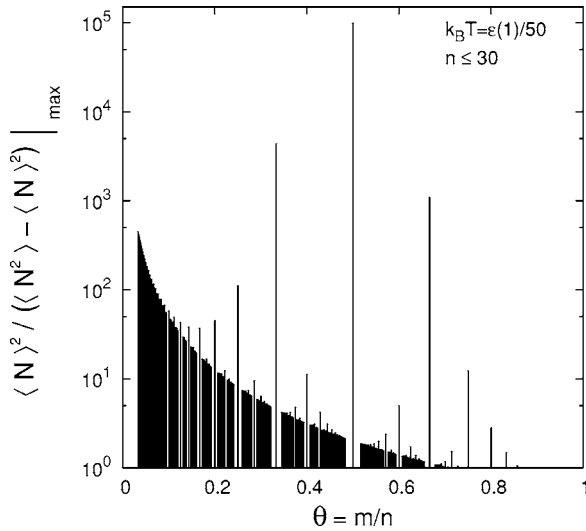


FIG. 10. Peaks of the static factor, Eq. (63), reached at coverages $\theta=m/n$ for the full devil's staircase system. For clarity, only peaks for coverages corresponding to $n \leq 30$ are displayed.

the expression (19) for the stability interval ΔP_q of the $\theta = 1/q$ phase for the staircase system.

Theoretical investigation of collective diffusion in the devil's staircase system is a formidable mathematical task and even full μ dependence of the static factor encounters unsurmountable difficulties. We may, however, assume that the inverse of the static factor is for this system proportional to the isothermal compressibility, like it is for the staircase system, i.e., it is given by the first line of Eq. (30) which, written in terms of particle number fluctuations gives $\mathcal{N} = (\langle N^2 \rangle - \langle N \rangle^2) / \langle N \rangle$. Then, a calculation similar to that leading to Eq. (31) results in the following expression for the maximum value of the static factor reached for μ at the center of the plateau corresponding to $\theta=m/n$ (as before, the overall factor $1/N$ is ignored in \mathcal{N})

$$\frac{\langle N \rangle^2}{\langle N^2 \rangle - \langle N \rangle^2} \Big|_{\max} = \frac{1}{2} \left(\frac{n}{m} \right)^2 e^{(1/2)\beta\Delta\mu(m/n)}. \quad (63)$$

Peak values of the static factor evaluated from Eqs. (63) and (62) for coverages $\theta=m/n$ with $n \leq 30$ are shown in Fig. 10. The same value of the parameter $k_B T / \varepsilon(1)$ corresponds to a different absolute temperature in the devil's staircase system than it does in the staircase system. Consequently, one should avoid making quantitative comparisons between results for both models even if complete expressions for the static and kinetic factor were available for the devil's staircase model. One may conclude from Fig. 10 that, after thermal broadening is accounted for, the coverage dependence of the static factor should show very sharp, almost singular peaks at coverages $\theta=m/n$ corresponding to the first few lowest values of n . Higher order peaks (higher n) would be smeared out into a background several orders of magnitude

below the dominant peak values. As we have seen for the staircase system the behavior of the kinetic factor might but does not have to result in the diffusion coefficient which follows closely the coverage dependence of the static factor. If it does, then fast reorganization of the system from one high-peak value structural phase to another one close to it may be expected even at very low temperatures when a small number of extra particles are added to the system. One might risk here a conclusion that the fact that such a fast self-organization is observed in a dense phase of Pb/Si(111)- $\sqrt{3} \times \sqrt{3}$ (Refs. 20 and 21), (a devil's staircase system not necessarily isomorphic with the Ising Model devil's staircase) indicates that the static factor has here a decisive influence on the coverage dependence of the collective diffusion coefficient.

VI. SUMMARY

We have generalized in this paper the proposed in Ref. 24 variational approach to collective diffusion. The generalization allows one not only to reproduce in a more transparent way than it was done in the original work all results obtained earlier for lattice gas systems with short-range interactions but it also allows one to investigate within the same theoretical framework systems with long-range repulsive interactions. In particular, coverage (i.e., the particle density) dependence of the collective diffusion coefficient is investigated here in detail for the originally proposed in Ref. 35 one-dimensional system with a staircaselike phase diagram. Within our variational approach in which factorization of the diffusion coefficient into the thermodynamic (static) and kinetic factor [cf. Eq. (1)] is not postulated both these factors have been now unambiguously identified and their dependence on pressure and coverage is investigated. As expected, the static factor exhibits as a function of coverage a series of sharp, almost singular peaks at coverages $\theta=1/q$ ($q=2,3,4,\dots$) for which the system is in a crystalline stable phase. The peaks are due to the low compressibility of such phases. At low temperatures the peak values are many orders of magnitude higher than the value of the static factor for $\theta \neq 1/q$ when the system is in an unstable liquid phase in which compressibility is high. The coverage dependence of the kinetic factor is more complicated and more interesting. Depending on details of the interactions of the migrating particle instantaneously at the top of the potential barrier between its initial and target adsorption site, i.e., the activated state interactions, the kinetic factor may exhibit: (i) singular minima at $\theta=1/q$, leading to a partial or complete compensation resulting in smooth coverage dependence of the diffusion coefficient, or (ii) it may have no singular structure at all resulting in the diffusion coefficient reflecting the singular structure of the static factor, or (iii) the kinetic factor may change in an almost steplike fashion at $\theta=1/q$ with the resulting diffusion coefficient showing similar discontinuities. Complete calculations of diffusion coefficient are not yet possible for a true devil's staircase system of Refs. 32, 34, and 33 with a fractal structure of the phase diagram (crystalline phases are for $\theta=m/n$ with m, n being integers). We speculate here, however, that the fast low temperature

self-reorganization between crystalline structures corresponding to infinitesimally different coverage phases observed for the Pb/Si(111) system indicates a singular coverage dependence of the diffusion coefficient listed above as (ii). In other words, the activated state interactions result most likely in the kinetic factor which is unable to compensate for the singularities present in the static factor.

ACKNOWLEDGMENTS

This work was partially supported by research grants from NSERC (the Natural Science and Engineering Research Council of Canada—Z.W.G.) and from KBN (Committee for Scientific Research of Poland, Grant No. 2 P03B 048 24—M.Z.K.). Extensive discussions with Dr. M. Tringides are gratefully acknowledged.

*Electronic address: zalum@ifpan.edu.pl

†Electronic address: gortel@phys.ualberta.ca

¹J. A. Venables, G. D. Spiller, and M. Hanbrücken, *Rep. Prog. Phys.* **47**, 399 (1984).

²A. Pimpinelli and J. Villain, *Physics of Crystal Growth* (Cambridge University Press, Cambridge, 1998).

³P. Jensen, *Rev. Mod. Phys.* **71**, 1695 (1999).

⁴J. V. Barth, *Surf. Sci. Rep.* **40**, 75 (2000).

⁵T. T. Tsong, *Surf. Sci.* **64**, 199 (2000).

⁶T. T. Tsong, *Prog. Surf. Sci.* **67**, 235 (2001).

⁷M. Giesen, *Prog. Surf. Sci.* **68**, 1 (2001).

⁸H. J. Kreuzer, in *Diffusion at Interfaces, Microscopic Concepts, Springer Series in Surface Science Vol. 12*, edited by M. Grunze, H. J. Kreuzer, and J. J. Weimar (Springer, New York, 1988), p. 63.

⁹H. J. Kreuzer and J. Zhang, *Appl. Phys. A: Solids Surf.* **51**, 183 (1990).

¹⁰H. J. Kreuzer, *J. Chem. Soc., Faraday Trans.* **86**, 1299 (1990).

¹¹A. A. Chumak and C. Uebing, *Eur. Phys. J. B* **9**, 323 (1999).

¹²R. Gomer, *Rep. Prog. Phys.* **53**, 917 (1990).

¹³A. Danani, R. Ferrando, E. Scalas, and M. Torri, *Int. J. Mod. Phys. B* **11**, 2217 (1997).

¹⁴T. Ala-Nissila, R. Ferrando, and S. C. Ying, *Adv. Phys.* **51**, 949 (2002).

¹⁵W. Teizer, R. B. Hallock, E. Dujardin, and T. W. Ebbesen, *Phys. Rev. Lett.* **82**, 5305 (1999); **84**, 1844 (2000).

¹⁶M. Hodak and L. A. Girifalco, *Phys. Rev. B* **64**, 035407 (2001).

¹⁷V. Meunier, J. Kephart, C. Roland, and J. Bernholc, *Phys. Rev. Lett.* **88**, 075506 (2002).

¹⁸T. Hasegawa and S. Hosoki, *Phys. Rev. B* **54**, 10300 (1996).

¹⁹A. Kirakosian, R. Bennewitz, F. J. Himpsel, and L. W. Bruch,

Phys. Rev. B **67**, 205412 (2003).

²⁰M. Hupalo, J. Schmalian, and M. C. Tringides, *Phys. Rev. Lett.* **90**, 216106 (2003).

²¹M. Yakes, V. Yeh, M. Hupalo, and M. C. Tringides, *Phys. Rev. B* **69**, 224103 (2004).

²²V. P. Zhdanov, *Elementary Physicochemical Processes on Solid Surfaces* (Plenum, New York, 1991).

²³D. A. Reed and G. Ehrlich, *Surf. Sci.* **102**, 588 (1981).

²⁴Z. W. Gortel and M. A. Załuska-Kotur, *Phys. Rev. B* **70**, 125431 (2004).

²⁵Ł. Badowski, M. A. Załuska-Kotur, and Z. W. Gortel, *Phys. Rev. B* **72**, 245413 (2005).

²⁶M. A. Załuska-Kotur, S. Krukowski, and Ł. A. Turski, *Surf. Sci.* **441**, 320 (1999).

²⁷M. A. Załuska-Kotur, S. Krukowski, Z. Romanowski, and Ł. A. Turski, *Surf. Sci.* **457**, 357 (2000).

²⁸M. A. Załuska-Kotur, A. Łusakowski, S. Krukowski, and Ł. A. Turski, *Surf. Sci.* **507-510**, 150 (2002).

²⁹M. A. Załuska-Kotur, S. Krukowski, and Ł. A. Turski, *Phys. Rev. B* **67**, 155406 (2003).

³⁰M. A. Załuska-Kotur, S. Krukowski, A. Łusakowski, and Ł. A. Turski, *Surf. Sci.* **566-568**, 210 (2004).

³¹C. Z. Zheng, C. K. Yeung, M. M. T. Loy, and Xudong Xiao, *Phys. Rev. B* **70**, 205402 (2004).

³²P. Bak and R. Bruinsma, *Phys. Rev. Lett.* **49**, 249 (1982).

³³M. H. Jensen, P. Bak, and T. Bohr, *Phys. Rev. Lett.* **50**, 1637 (1983).

³⁴P. Bak, *Rep. Prog. Phys.* **45**, 587 (1982).

³⁵V. V. Slavin and A. A. Slutskin, *Phys. Rev. B* **54**, 8095 (1996).

³⁶M. A. Załuska-Kotur and Z. W. Gortel, *Phys. Rev. B* **72**, 235425 (2005).

³⁷R. Kutner, *Phys. Lett.* **81A**, 239 (1981).